Statistical Data Analysis of the Aurora Electrons and Thermal Ions for Spacecraft Charging Analysis

Takamitsu Hamanaga and Mengu Cho
Department of Electrical Engineering, Kyushu Institute of Technology, 1-1 Sensui-cho Tobata-ku Kitakyushu, 804-8550, Japan

Polar Earth orbit (PEO) is a peculiar orbit where energetic auroral electrons and low-temperature ionospheric plasma coexist. There is a risk of charging and subsequent arcing in PEO, which was demonstrated unfortunately by the total loss of ADEOS-II satellite in 2003. Charging in PEO must be properly assessed in the early satellite design phase by a spacecraft charging analysis tool. The plasma environment, namely its density and energy, is the crucial parameter for the spacecraft charging analysis. The balance between the auroral electrons and the low temperature ionospheric ions determine the charging potential of a PEO satellite. We statistically analyzed the environmental condition in PEO using the data of auroral electrons and thermal ions measured by DMSP (Defense Meteorological Satellite Program) satellites. Probability of a given combination of current densities of auroral electrons and thermal ions has been derived. The energy spectrum of the auroral electrons are also classified into several types and correlation with the thermal ions is analyzed. Combinations of the plasma parameters used by a spacecraft charging simulation software have been identified and database regarding the probability of occurrence of each combination has been formulated.

I. Introduction

Compared to spacecraft charging in GEO, charging in LEO has not been given serious consideration because of presence of high density and low temperature ionospheric plasma. The balance of negative and positive currents to the spacecraft determines its potential with respect to the surrounding plasma. If a spacecraft is in low-inclination orbit that does not cross with the aurora zone, defined as the region between 60 and 75 degrees of magnetic latitude (MLAT), the ionspheric plasma dominates the current and the spacecraft potential is within the solar array power generation voltage[1].

Polar Earth orbit (PEO) that crosses the aurora zone is a peculiar orbit where the low-temperature plasma and energetic auroral electrons coexist. Therefore, a PEO spacecraft may charge to hundreds or thousands of volts negative when the density of thermal ions is reduced or the flux of auroral electrons become large[2,3]. In such a situation, if a potential difference between the spacecraft body and the spacecraft insulator material exceeds the arc inception threshold, an arc occurs. This may lead to a serious accident. In October 2003, a Japanese Earth observation satellite, ADEOS-II, suffered fatal power system failure because of sustained arc in cable harness phenomena triggered by charging of ungrounded thermal insulator by auroral electrons[4]. Since the accident of ADEOS-II, Japanese space sector takes spacecraft charging in PEO very seriously.

To prevent such an accident, charging in PEO must be properly assessed in the early satellite design phase by a spacecraft charging analysis tool. If the charging analysis predicts that the probability of arcing in orbit cannot be ignored, proper ground tests must be carried out[5,6]. In the Japanese space sector, JAXA decided to develop MUSCAT (Multi-Utility Spacecraft Charging Analysis Tool) [7] based on the lessons learned from the ADEOS-II failure. There are several ways of using the charging simulation code. One is to know whether the spacecraft reaches the critical charging situation where arcs are inevitable by simulating the worst plasma condition. Another is to know how many arcs a spacecraft suffers during the total lifetime. The later information is used to plan the ground test and assess the cumulative effects, such as surface deterioration or solar cell degradation, at the end of life[8].

Knowing the correct plasma environment a spacecraft encounters in orbit is very important to make use of the charging simulation code. Not only the worst condition but also statistical distribution of the plasma parameters are important if we like to derive the statistical prediction from the charging analysis and the ground test. The purpose of the present paper is to formulate a database regarding the PEO plasma environment suitable for the charging simulation code.

MUSCAT can simulate the spacecraft plasma interaction by modeling the ionosphere plasma by Maxwellian plasma and the auroral electron either by a single Maxwellian or a double Maxwellian plasma. In the MUSCAT simulation, the auroral electrons are injected from the numerical boundary donwnward only along the magnetic field line[8]. Therefore, we need at least a combination of ionospheric plasma density, auroral electron density and its temperature. In Ref.9 Cho et al carried out statistical analysis of GEO plasma environment using the data measured by LANL (Los Alamos National Laboratory) satellites. In Ref.9, the probability of each combination of electron density, electron temperature, ion density and ion temperature was derived assuming the GEO plasma was made by single Maxwellian electrons and ions. In the present paper, we carry out statistical analysis similar to Ref.9 using the data measured by DMSP (Defense Meteorological Satellite Program) satellites.

In the second section, we describe the DMSP data we used. In the third section, we describe the result of correlation analysis on the auroral electron current and thermal (ionospheric) ion current from 1996 to 2003.

II. Data Description

The data we used comes from data of SSJ/4 (precipitating electron and ion sensor), and SSIES (Special Sensor for Ion Scintillation monitor) onboard DMSP[#]. DMSP is a group of satellites orbiting the Earth at approximately 840 km altitude with 99° inclination and 101 minute orbital period. More than two DMSP satellites are always operated. Each DMSP satellite is classified by a number like F6 or F7 and so on.

SSJ/4 measures the energy spectrum of precipitating particles between 30 eV and 30 keV using 20 channels and records each channel every second[#]. Each channel covers a specific energy band and is logarithmically spaced between 30 eV and 30 keV. Each channel records the magnitude of the particle energy flux. We calculate the current density of the auroral electrons using the data of SSJ/4 according to the following process.

We assume that the velocity distribution of the energetic electrons is isotropic within 2π solid angle, which is defined by $0 < \Phi < 2$ and $0 < \theta < /2$, in polar coordinate shown in Figure 1.

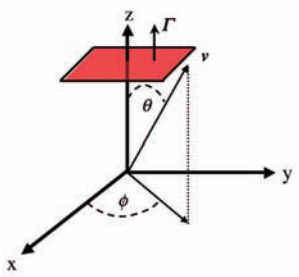

Fig.1 Particle flux and velocity vector

The energy flux in polar coordinates is given by the following equation.

$$\begin{aligned} &EnergyFlux(J/s/m^2) \\ &= \int_{v_{\min}}^{v_{\max}} \int_0^{\pi/2} \int_0^{2\pi} \left(\frac{1}{2}mv^2\right)(v^2 \sin\theta d\theta d\phi) dv\, f(v) v \cos\theta \\ &= \pi \int_{v_{\min}}^{v^{\max}} \frac{1}{2} m v^5 f(v) dv \\ &= 2\pi \Gamma_{flux} \end{aligned} \quad (1)$$

where Γ_{flux} is the value observed by SSJ/4 and v is a speed that corresponds to each channel energy.

The solid angle of 2 is used assuming that particles are unidirectional along the magnetic field lines. From Eq (1), the distribution function f(v) is given by the following equation (2).

$$f(v) = \frac{2\Gamma_e(E)}{v^3 \frac{1}{2} m v^2} \bullet \frac{1}{v_{i,\max} - v_{i,\min}} \quad (2)$$

where $v_{i,min}$ is the velocity corresponding to the minimum energy that a channel i can observe, $v_{i,max}$ is the velocity corresponding to the maximum energy that a channel i can observe and E is the channel energy. One might argue that energetic electrons in aurora may not be isotropic, and more oriented along the magnetic field line. As SSJ/4 measures only the energy flux in a limited solid angle, it is very difficult to estimate the angular width of the precipitating electrons. As the first step we multiply Γ_{flux} by 2 as in Eq (1) and it should be noted that this treatment leads to overestimation of the electron density and current to a certain degree.

We can derive the density by integrating the distribution function of electrons.

$$n = 4\pi \int_{v_i,\min}^{v_{i,\max}} f(v) v^2 dv \quad (3)$$

Average energy and current density is derived from the density and the distribution function. They are

$$< \frac{mv^2}{2} >= \frac{2\pi m \int_{v_{i,\min}}^{v_{i,\max}} f(v) v^4 dv}{n} \quad (4)$$

[#] http://www.ngdc.noaa.gov/dmsp/dmsp.html

where $<\frac{mv^2}{2}>$ is the average energy. The total current density i is given by

$$i = e < nv >= \int_{v_{i,\min}}^{v_{i,\max}} \int_0^{\pi/2} \int_0^{2\pi} e(v\cos\theta)(v^2 \sin\theta d\theta d\phi) dv f(v) \quad (5)$$
$$= e\pi \int_{v_{i,\min}}^{v_{i,\max}} v^3 f(v) dv$$

SSIES measures density, temperature, and velocity of the background thermal plasma. Sampling rate is 4 second[15]. We used the data of the thermal ion density.

The SSJ/4 data was obtained from the website* of "The Johns Hopkins University Applied Physics Laboratory" and SSIES data was obtained from the website§ of "DMSP SSIES Data Distribution Website". The data is from January, April, July, and October in 1996, 2000, and 2003 so that we can cover the maximum, the minimum and the middle of one solar cycle and four seasons. We analyzed only the data observed at the same time by both SSJ/4 and SSIES in the magnetic latitude between 60° and 75° in the southern and northern hemisphere. Number of data points we used is listed in table 1.

Table.1 Number of data points between 60° and 75° MLAT. (North and South) used in the analysis of sections 4 and 5.

	Jan	Apr	Jul	Oct	Satellites
96	266975	256811	217662	280040	F12,13
00	453929	500041	371375	372608	F12,13,14,15
03	234357	261944	255331	226339	F13,14,15

III. Concurrent Statistical Data Analysis of the Current Density of Auroral Electrons and Thermal Ions

In this section, we first classify the scale of the aurora into 5 types, Extreme, Severe, Strong, Moderate, and Weak (table 2). We made no distinction between the northern and the southern hemisphere. Moderate is the most probable type as scaling of the aurora. When the aurora becomes active, the scale changes in the order of Strong, Extreme and Severe, where the current to spacecraft is dominated by the auroral electrons. Weak is the case when auroal electrons hardly precipitate into the spacecraft.

Table 3 shows the probability that a spacecraft encounters a certain aurora condition at daytime or at nighttime in magnetic local time (MLT). Extreme and Severe show no significant dependence on MLT. Strong tends to occur more during nighttime than daytime. In addition, the probability of Strong type aurora becomes higher during the solar maximum (2000 and 2003) than the solar minimum (1996) (see Table 4).

Figure 2 shows the ion density in July 1996 and in July 2000. In July, the northern hemisphere is always illuminated. Therefore the ion density is high and stable. In contrast, the southern hemisphere is not illuminated, which makes the ion density low and fluctuating.

We classified the ion density into 3 types, Rare, Medium, and Dense (Table.5). The ion current was calculated by multiplying the density by 8 km/s, the orbital velocity. When the ion density becomes Rare, the auroral current of Strong, Severe, and Extreme exceeds the ion current. Figure 3 shows the relationship between the scale of the aurora and the scale of the thermal ion in the southern hemisphere in July 2000 between 21 MLT and 24 MLT. The southern hemisphere is not illuminated in July. Table 6 shows the probability that a spacecraft encounters a certain plasma environment in July 2000 in the southern hemisphere between 21MLT and 24MLT. The ion density becomes lower if the scale of the aurora becomes weaker and the ion density becomes higher if the scale of the aurora becomes stronger. This is caused by the increase of the ion density due to ionization of the atmosphere by the energetic auroral electrons. In the same way, the northern hemisphere in January have the same tendency.

The ion density in the illuminated region doesn't have this tendency, because the effect of the solar illumination is much stronger than the effect of ionization by auroral electrons.

From Tables 2 and 6, it is found that Severe and Extreme aurora scale and even Strong if accompanied by the ion density less than 8×10^8 m^{-3} may lead to serious negative charging of a spacecraft body. In Table 6 those cases are enclosed in the thick line. The total percentage of those charging cases is 0.84% in July 2000 in the southern hemisphere between 21MLT and 24MLT. A major part of this charging case is dominated by the Strong scale aurora. Thus, most charging event occur due to the decrease of ion density rather than the increase of the auroral current. Although it is very rare, less than 0.01%, in the Extreme case, spacecraft may charge to over -10kV because the auroral electrons energy is above 10keV.

* http://sd-www.jhuapl.edu/Aurora/dataset_list.html
§ http://cindispace.utdallas.edu/DMSP/

Table 2. Definition of aurora scale and its conditions.

Scale	Current Density (A/m^2)	Average Energy (keV)
Extreme	$>10^{-4}$	>10
Severe	$>10^{-4}$	<10
Strong	10^{-6}~10^{-4}	
Moderate	10^{-8}~10^{-6}	
Weak	$<10^{-8}$	

Table 3. Scale of aurora and probability (%) in 9~12 MLT and 21~24 MLT.

Scale	9~12 MLT			21~24 MLT		
	1996	2000	2003	1996	2000	2003
Extreme	0	0.006	0	0	0.005	0
Severe	0.08	0.14	0.4	0.09	0.16	0.22
Strong	9	22	34	34	41	53
Moderate	91	78	65	58	57	45
Weak	0.02	0.06	0.9	8	1.7	2.1

Table 4. Probability of each aurora scale (%) .

Scale	Probability (%)		
	1996	2000	2003
Extreme	0.0002	0.0035	0.0001
Severe	0.08	0.14	0.23
Strong	24	35	41
Moderate	73	64	57
Weak	2.5	0.5	1.1

Table 5. Scale of thermal ion and its conditions.

Scale	Current Density (A/m^2)	Density (m^{-3})
Rare	$<10^{-6}$	$<8\times10^{8}$
Medium	10^{-6}~10^{-4}	8×10^{8}~8×10^{10}
Dense	$>10^{-4}$	$>8\times10^{10}$

Table 6. Statistical correlation probability(%) between ion and electron current. (July 2000 in the southern hemisphere between 21MLT and 24MLT)

	Weak	Moderate	Strong	Severe	Extreme
Rare	0.11	0.69	0.64	0.003	0.0
Medium	1.1	54	40	0.17	0.005
Dense	0.023	1.6	2.1	0.021	0.003

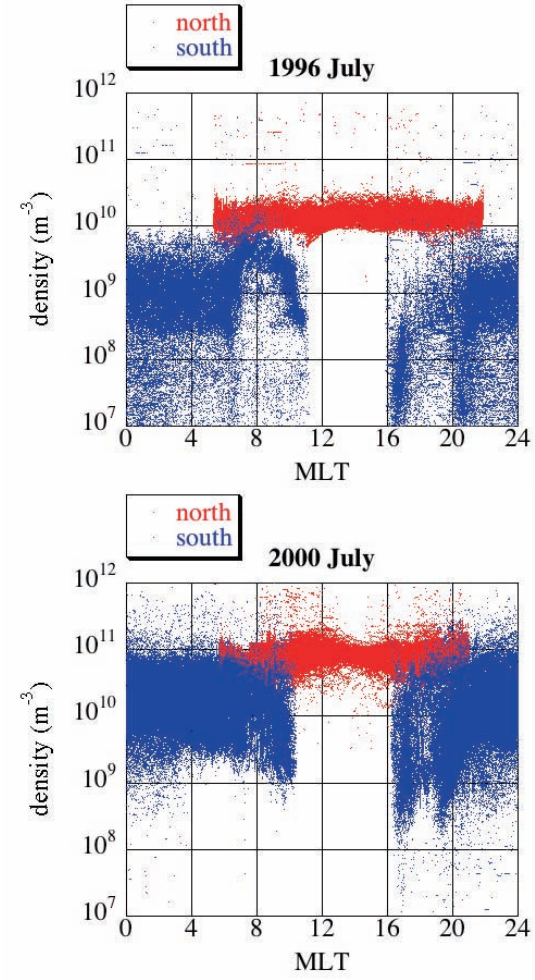

Fig.2. Relation between thermal ion density and MLT in July.(top:1996,July,north, 2nd low:1996,July,south, 3rd low:2000,July,north, bottom: 2000,July,south)

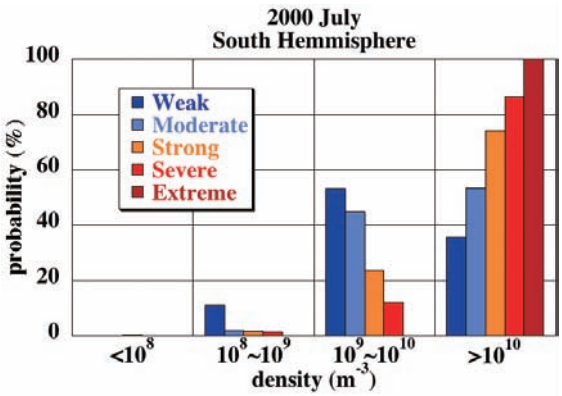

Fig. 3. Relation between the scale of the aurora and the ion density (July 2000 in the southern hemisphere between 21MLT and 24MLT.)

Table 7 shows the probability of the auroral current exceeding the ion current. The percentage of Strong type aurora to each probability is listed in the parentheses. For an example, in October in the southern hemisphere in 1996 between 0 MLT and 3 MLT, the probability of the auroral electron current exceeding the thermal ion current is 0.07%. In the 0.07%, 22.2% corresponds to Strong scale aurora and the rest corresponds to Severe and Extreme aurora. The charging probability due to the decreasing ion density is evident during the solar minimum in January 1996 in the northern hemisphere and in July in the southern hemisphere. In contrast, the charging probability due to the active aurora is evident during the solar maximum in July 2000 in the northern hemisphere where no Strong case exists. For the case of charging due to the active aurora, the ratio of Extreme and Severe cases in the probability increases compared to charging due to the decreasing ion density.

Table 7. Probability of auroral current exceeding ion current (%)

MLT	1996							
	North				South			
	Jan	Apr	Jul	Oct	Jan	Apr	Jul	Oct
0~3	n/a	n/a	n/a	n/a	0.02(0.0)	8.08(99.0)	28.13(99.8)	0.07(22.2)
3~6	19.53(100)	0.12(14.3)	0.22(14.3)	1.86(95.2)	0.04(0.0)	4.50(98.5)	16.77(99.8)	0.06(18.8)
6~9	15.10(99.1)	0.16(0.0)	0.11(0.0)	1.80(92.9)	0.09(0.0)	5.80(99.1)	8.84(99.5)	0.17(62.8)
9~12	2.04(96.6)	0.01(2.6)	0.13(0.0)	0.29(54.9)	0.00(0.0)	0.44(93.6)	2.27(100)	0.01(0.0)
12~15	1.21(90.1)	0.16(0.0)	0.11(0.0)	0.21(11.1)	n/a	n/a	n/a	n/a
15~18	2.10(93.0)	0.09(0.0)	0.05(0.0)	0.24(68.1)	0.01(0.0)	7.56(99.9)	7.70(100)	0.35(97.4)
18~21	4.93(99.1)	0.13(0.0)	0.04(0.0)	1.00(87.0)	0.10(79.2)	10.37(99.5)	13.96(99.9)	1.80(95.9)
21~24	5.17(98.6)	0.07(0.0)	0.01(0.0)	4.09(95.5)	0.09(4.5)	13.66(99.4)	18.42(99.4)	0.47(81.4)

MLT	2000							
	North				South			
	Jan	Apr	Jul	Oct	Jan	Apr	Jul	Oct
0~3	n/a	n/a	n/a	n/a	0.06(0.0)	0.12(0.0)	0.39(48.9)	0.09(0.0)
3~6	0.07(0.0)	0.09(0.0)	0.27(0.0)	n/a	0.07(0.0)	0.05(3.4)	0.16(10.1)	0.11(0.0)
6~9	0.18(3.2)	0.11(0.0)	0.25(0.0)	0.22(0.0)	0.14(0.0)	0.09(0.0)	0.18(2.4)	0.18(0.0)
9~12	0.13(0.0)	0.16(0.0)	0.28(0.0)	0.08(0.0)	0.18(0.0)	0.08(0.0)	0.23(24.0)	0.10(0.0)
12~15	0.43(0.0)	0.34(0.0)	1.11(0.0)	0.26(0.0)	n/a	n/a	n/a	n/a
15~18	0.19(1.4)	0.07(0.0)	0.32(0.0)	0.12(0.0)	0.03(0.0)	0.26(96.4)	0.91(92.7)	0.10(0.0)
18~21	0.15(0.0)	0.07(0.0)	0.18(0.0)	0.10(0.0)	0.10(0.0)	0.98(97.0)	1.31(90.1)	0.05(5.9)
21~24	0.09(0.0)	0.21(0.0)	0.00(0.0)	0.92(0.0)	0.16(0.0)	0.17(36.5)	0.84(75.9)	0.18(0.0)

MLT	2003							
	North				South			
	Jan	Apr	Jul	Oct	Jan	Apr	Jul	Oct
0~3	n/a	n/a	n/a	n/a	0.16(0.0)	0.08(17.6)	2.25(89.8)	0.09(0.0)
3~6	0.00(0.0)	n/a	n/a	n/a	0.08(0.0)	0.06(0.0)	0.92(86.7)	0.17(0.0)
6~9	0.23(1.2)	0.15(0.0)	0.43(0.0)	0.47(0.0)	0.17(0.0)	0.16(7.7)	1.32(66.7)	0.38(0.0)
9~12	0.37(0.0)	0.21(0.0)	0.72(0.0)	0.27(1.6)	0.69(0.0)	0.05(0.0)	2.03(60.0)	0.09(0.0)
12~15	0.90(2.9)	0.43(0.0)	0.95(0.0)	0.32(0.0)	0.00(0.0)	n/a	n/a	n/a
15~18	0.28(3.5)	0.15(0.0)	0.39(0.0)	0.17(0.0)	0.07(0.0)	2.64(99.6)	6.15(00.6)	0.38(0.0)
18~21	0.17(0.0)	0.07(0.0)	0.20(0.0)	0.38(0.0)	0.07(0.0)	2.24(97.5)	5.56(98.0)	0.18(11.6)
21~24	n/a	n/a	n/a	n/a	0.23(0.0)	0.44(70.2)	3.52(91.3)	0.20(0.0(0.0))

IV. Database for Spacecraft Charging Anaysis Parameter for MUSCAT

Finally, we formulate the database of input parameters of PEO plasma environment suitable for a parametric run by a spacecraft charging analysis tool such as MUSCAT.

In MUSCAT, the input plasma parameters for PEO analysis are the current density and average energy of aurora and surrounding thermal plasma density. The aurora electrons are modeled by a Maxwellian distribution. The temperature of surrounding plasma may vary between 0.1 to 0.2eV. Because the difference is negligible compared to the possible charging potential and the thermal speed is negligible compared to the orbital velocity, we fix the temperature to 0.2eV.

The purpose of the parametric run is to investigate as many cases as possible to derive the number of charging events in orbit. By knowing the time for the differential voltage between spacecraft surface insulator and the spacecraft body to reach the threshold for primary arc inception, we can also derive the expected number of primary arcs in orbit. This practice was once carried out for a GEO satellite in Ref.13. We can derive those numbers if we know the probability of occurrence for each set of the plasma environment parameters.

To formulate the database of possible combinations of the plasma parameters, we used the DMSP data of January, April, July and October in 1996, 2000, and 2003 between 60° MLAT and 75° MLAT in both hemispheres. In this way, we can cover four seasons in the northern and southern aurora zones during the solar maximum (2000), the solar minimum (1996) and the intermediate time (2003). To resolve the local time dependence, we divided the data into 8 MLT zones that have duration of 3 hours. In this way, the number of temporal and spatial combinations are 3x4x8x2=192 cases.

At each of 192 cases, we further divide the plasma environment depending on the aurora current density, average energy, spectra and thermal ion density. The ranges of each plasma parameter used to categorize are shown in table 8. For the aurora current density, we combined all the cases below 10^{-6}A/m^2 because the current density below 10^{-6}A/m^2 has little effect on negative charging. When we carry out the simulation for the case representing the aurora current density less than 10^{-6}A/m^2, we choose the aurora current density $1x10^{-6}$A/m^2 as the input value for the simulation. For the case of aurora current density from $1x10^{-6}$ to $1x10^{-5}$A/m^2, we choose $1x10^{-5}$A/m^2 as the input value of the aurora current density. The other input values are listed in Table 7. For the thermal plasma density above 10^{10}m^{-3} is combined into $1x10^{10}$m^{-3} as the dense plasma relaxes the negative charging. Choosing the aurora current density at the upper-bound of each range and the thermal ion density at the lower bound gives more cases of negative charging, leading to the conservative (safe-side) estimate on the number of charging events in orbit.

We divided the aurora spectrum into three cases to consider the correlation between spectrum of auroral electrons and thermal ions. We represent the energy flux by two-Maxwellian distribution. The formulation is following.

$$flux(\varepsilon) = M_1\left(\frac{1}{2\pi}\right)^{\frac{3}{2}}\sqrt{\frac{kT_1}{m}}\left(\frac{\varepsilon}{kT_1}\right)^{\frac{3}{2}}\exp\left(-\frac{\varepsilon}{kT_1}\right)$$

$$+M_2\left(\frac{1}{2\pi}\right)^{\frac{3}{2}}\sqrt{\frac{kT_2}{m}}\left(\frac{\varepsilon}{kT_2}\right)^{\frac{3}{2}}\exp\left(-\frac{\varepsilon}{kT_2}\right)$$

where $flux(\varepsilon)$ is the energy distribution function, M_1 and M_2 are electron density and T_1 and T_2 are electron temperature. T_1 is greater than T_2. Spectra are represented by the Maxwellian distribution of low temperature T_1 and high temperature T_2. We consider 3 cases. Case1; $M_1 \times 10 < M_2$, case2; $M_1 \times 10 \geqq M_2$ and $M_2 \times 10 \geqq M_1$, and case3; $M_1 > M_2 \times 10$. Case1 is the environment dominated by high energy electrons. Case2 is the environment that various energy electrons are precipitating. Case3 is the environment dominated by low energy electrons

We fitted M_1, M_2, T_1, and T_3 to the observational value of SSJ/4 using genetic algorithm fitting. The range for M_1 and M_2 are from 10^4m^{-3} to 10^{10}m^{-3}. The range for T_1 is from 10eV to 1keV. The range for T_2 is from 1keV to 80keV. Figure 4 shows the observational value and fitting value of case1, case2, and case3.

If the spectrum is categorized as the Case1, the temperature is further divided into the four cases listed in Table 8. The aurora electrons are modeled by a single Maxwellian with the temperature listed in the next column in Table 8. Likewise, if the spectrum is categorized as the Case3, the temperature is further divided into three cases. If the spectrum is categorized as the Case2, we multiply the average energy defined by Eq. (4) by 2/3 to obtain single temperature to be used to model the electron energy distribution by a single Maxwellian. For the case where the aurora current density is below 10^{-6}A/m^2, we neglect the difference of the aurora energy spectrum and treat all the spectrum type as case 2 for simplicity.

For each thermal plasma density, the number of combination for the aurora current density and temperature is 8+3x16=56. Therefore, the total number of combination for the plasma parameter is 4x56=224. Therefore, the total number of combination considering the solar activity, the season, the local time, the hemisphere and the plasma parameters is

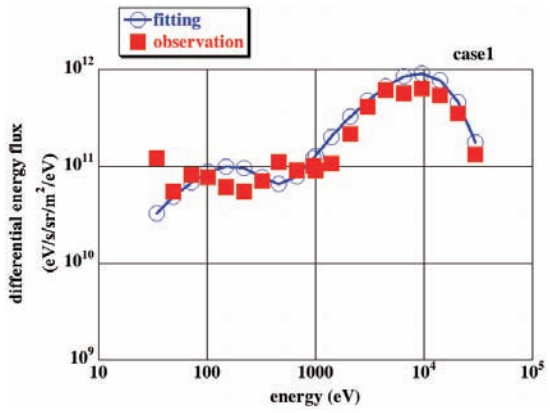

(a) case1

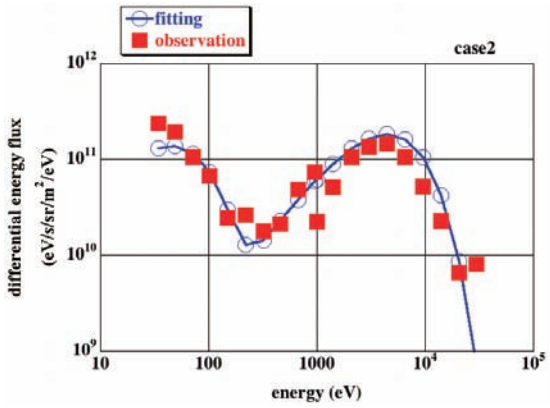

(b) case2

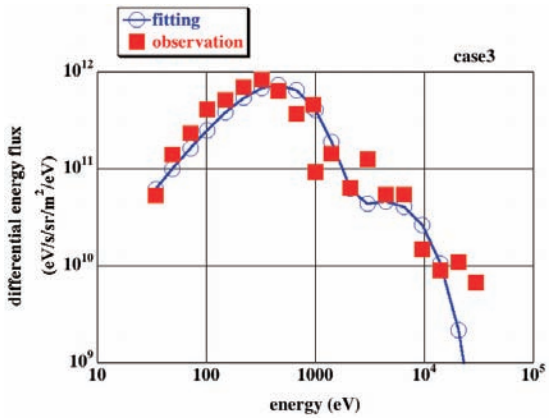

(c) case3

Fig 4. Fitting spectrum

192x224=43008. We calculate the probability of occurrence of each of 224 combinations of plasma parameters at each case of the 192 temporal and spatial combinations. Among the 192 temporal and spatial combinations, unfortunately, there are cases where no DMSP data is available. We compensate the no data region using adjacent time zones. No data regions are 0~3MLT, 3~6MLT, and 21~24MLT in the northern hemisphere and 12~15MLT in the southern hemisphere. Figure 2 shows little dependency on MLT, so we compensated no data regions considering only the aurora activity referring to the probability of 'the worst case' in Ref.10. Data of 0~3MLT, 3~6MLT, and 21~24MLT in the northern hemisphere are compensated by data of 18~21MLT, 15~18MLT, 18~21MLT in the northern hemisphere respectively. Data of 12~15MLT in the southern hemisphere is compensated by data of 9~12MLT in the southern hemisphere.

Among the 43008 combinations, there are cases where the probability of occurrence is zero. After we delete the cases with zero probability, there are only 2858 cases left. For parametric run, we can reduce the number of simulation to 930 cases because we have only to consider the plasma density, the auroral current, the temperature, time region, and the hemisphere in the calculation. We can further reduce the number of simulation by ignoring the cases where little negative charging is expected with the aurora current density much lower than the thermal ion current density. Deleting such cases, the number of simulation necessary is approximately 400. If we can finish each simulation case in 15 minutes, all the simulations can be done in less than 5 days.

V. Conclusion

It is necessary to characterize the plasma parameters in PEO to correctly access the risk of spacecraft charging in orbit and draft an appropriate ground test plan if necessary. Whether a spacecraft in PEO suffers serious negative charging beyond the solar array power generation voltage, depends on the balance between energetic auroral electrons and ionospheric ions. The plasma conditions have statistical distribution depending on the solar activity, orbital position, season and local time. To carry out quantitative analysis to derive the probability of serious charge events in orbit, we need to know not only the worst-case condition but also the probability of occurrence of each combination of the plasma parameters. In the present paper, we have statistically analyzed the current density of the aurora and background thermal ion in PEO using data of DMSP to produce a database suitable for series of spacecraft charging simulations to derive the number of charging events and the estimated number of primary arcs in orbit.

The statistical analysis of DMSP SSJ/4 and SSIES data revealed that during the solar maximum, the probability of negative charging due to active aurora rises. During the solar minimum, the probability of negative charging due to decrease of ion density rises especially in the southern hemisphere.

We have formulated a database to be used as input parameters of spacecraft charging simulation code,

MUSCAT. We have derived the probability of occurrence of each combination of season, solar activity, hemisphere, magnetic local time, auroral current density, ionospeheric ion density and auroral electron temperature. In the database, we have divided the seasons into 4, the solar activity into 3 levels, the hemispheres into south and north, the magnetic local to 8 time zones, the auroral current density into 4 levels, the ion density into 4 levels and the auroral electron temperature into 16 levels. Although the total number of combinations is more than 50,000, if we consider only the cases with non-zero probability of occurrence and possibility of auroral current density exceeding the ionospheric ion density, the number of case reduces to 400.

Our next task is to carry out the simulation runs of the 400 cases by MUSCAT and calculate the spacecraft charging potential and time for the differential voltage to reach the arcing threshold for each case.

In the present paper, the data we used for the statistical analysis is limited to DMSP. Therefore, strictly speaking the database we formulated is applicable only to the altitude of 840km. Correction would become necessary whenever we carry out the charging simulation for spacecraft in a different altitude. We have used only a limited amount of DMSP data to carry out the concurrent analysis of the auroral current and the ionospheric ion density. In future, it is necessary to refine the accuracy of database by increasing the number of observation data involved.

Acknowledgments

We thank Dr. Patrick Newell of Johns Hopkins University Applied Physics Laboratory for helping us analyze the data of SSJ/4.

References

[1]D. E. Hastings and H. Garrett, “Spacecraft-Environmental Interactions”, *Cambridge Univ.Press*, New York, 1996.

[2]P. C. Anderson, “A Survey of Surface Charging Events on the DMSP Spacecraft in LEO”, Proceedings of 7th Spacecraft Charging Technology Conference, ESA, SP476, 2001, pp.331-336.

[3] J. E. Wahlund, L. J. Wedin, T. Carrozi, A. I. Eriksson, B. Holback, L. Andersson and H. Laakso, “Analysis of Freja Charging Events: Statistical Occurrence of Charging Events”, *ESA TECHNICAL NOTE*, SPEE-WP130-TN, 1999.

[4]S. Kawakita, H. Kusawake, M. Takahashi, H. Maejima, T. Kurosaki, Y. Kojima, D. Goto, Y. Kimoto, J. Ishizawa, M. Nakamura, J. Kim, S. Hosoda, M. Cho, K. Toyoda and Y. Nozaki, “Investigation of an Operational Anomaly of the ADEOS-II Satellite”, 9th SCTC, Tsukuba, 2005.

[5]Mengu Cho, Jeong-ho Kim, Satoshi Hosoda, Yukishige Nozaki, takeshi Miura, and Takanori Iwata, “Electrostatic Discharge Ground Test of a Polar Orbit Satellite Solar Panel” IEEE Transaction on Plasma Science, Vol.34, pp.2011-2030, 2006

[6]Kazuhiro Toyoda, Hirokazu Masui, Takanobu Muranaka, and Mengu Cho, Tomoyuki Urabe, Takeshi Miura, and Shirou Kawakita, Yuichiro Gonohe and Tooru Kikuchi, ”Esd Ground Test of Solar Array Coupons for a Greenhouse Gases Observing Satellite in PEO”10th Spacecraft Charging Technology Conference, Biarritz, France, June 2007

[7]Takanobu MURANAKA, Shinji HATTA, Jeongho KIM,Satoshi HOSODA, Koichiro IKEDA, Mengu CHO, Hiroko O. UEDA, Kiyokazu KOGA, Tateo GOKA, ”Final Version of Multi-Utility Spacecraft Charging Analysis Tool (MUSCAT)”, 10th Spacecraft Charging Technology Conference, Biarritz, France, June 2007

[8]Mengu CHO**,** “Status of ISO Standardization Efforts of Solar Panel ESD Test Methods”, 10th Spacecraft Charging Technology Conference, Biarritz, France, June 2007

[9]Mengu Cho, Shirou Kawakita, Masao Nakamura, Masato Takahashi, Tetsuo Sato, Yukishige Nozaki, “Number of arcs estimated on solar array of a geostationary satellite” 2005, Journal of Spacecraft and Rockets, vol.42 no.4, pp.740-748

[10]Takamitsu Hamanaga, Shinji Hatta, Mengu Cho, “Analysis of the Plasma Environment in Polar Earth Orbit Using Data of Defense Meteorological Satellite Program”, The 25th International Symposium on Space Technology and Science, 2006

Table 8. Range and input value of each case of plasma parameters

Range of aurora current density (A/m^2)	Input value of aurora current density (A/m^2)	Range of thermal plasma density (m^{-3})	Input value of thermal plasma density (m^{-3})	Aurora electron spectrum and temperature (eV)		Input value of aurora electron temperature (eV)
~$1x10^{-6}$	$1x10^{-6}$	~$1x10^{8}$	$5x10^{7}$	Case 1	1000~2000	2000
$1x10^{-6}$~$1x10^{-5}$	$1x10^{-5}$	$1x10^{8}$~$1x10^{9}$	$1x10^{8}$		2000~4500	4500
$1x10^{-5}$~$1x10^{-4}$	$1x10^{-4}$	$1x10^{9}$~$1x10^{10}$	$1x10^{9}$		4500~10000	10000
$1x10^{-4}$~	$5x10^{-4}$	$1x10^{10}$~	$1x10^{10}$		10000~20000	20000
					20000~	30000
				Case 2	10~200	200
					200~450	450
					450~1000	1000
					1000~2000	2000
					2000~4500	4500
					4500~10000	10000
					10000~20000	20000
					20000~	30000
				Case 3	10~200	200
					200~450	450
					450~1000	1000